Hamiltonian Truncation Applied to Lattice ϕ^4 Theory

Advised by Dr. Markus Luty, UC Davis Physics Dept. (QMAP)

Joey Takach

A paper written in completion of the
UC Davis + NSF REU Program

Department of Physics
University of California, Davis
February 4, 2024

Abstract

In this project, we seek to further develop the method of Hamiltonian truncation to numerically study the ϕ^4 scalar QFT on the lattice. By truncating the infinite Hilbert space to a finite one, we can approximate the vacuum and low energy states of the theory. Using this information, we will demonstrate the possibility of interesting physical measurements achievable through this method that cannot be obtained analytically, such as an estimate of the critical coupling in the continuum limit. We will then compare our results with other implementations of Hamiltonian truncation as well as other numerical approaches with the same goal.

Contents

List of Figures

Chapter 1

Introductory Material

1.1 Introduction

Quantum field theory (QFT) gives us the most comprehensive and detailed understanding of fundamental physics that is currently possible. It has led humanity to the most detailed agreement of theory and experiment ever achieved, through its implementation in quantum electrodynamics, or QED [2]. However, this success is due in part to the weakly interacting nature of QED; that is, the particles involved in the theory do not interact with each other very strongly [3]. Feynman and Schwinger taught us to exploit this weak coupling by calculating quantities of interest by means of a perturbative expansion in the small coupling parameter α, the fine structure constant [4, 5]. But once we compare to the strongly coupled theory of nuclear physics described by quantum chromodynamics (QCD), the relevant coupling constant is very large at energy scales we would like to study, and we can no longer use the same perturbative methods with success [3]. With QCD in particular, it is the behavior over large distances where our understanding breaks down, while at short distances we have asymptotic freedom [6]. In order to better understand these strongly coupled theories, at least for now, we must resort to approximation methods that give us a precise picture of the mechanisms at play [7, 8, 9, 10].

1.2 Background

Hamiltonian truncation is a numerical method to study strongly coupled QFT's. But more generally, it is a method that can be applied to any quantum theory with a continuous degree of freedom. The main goal is to take an unsolvable (infinite dimensional) Hamiltonian of interest, H, and to find a division of it into an exactly solvable part (H_0) and an interacting part (V), much like perturbation theory: $H = H_0 + V$. We can use our exactly solvable H_0 to construct a basis for the Hilbert space, and then take a finite subset of that to make our truncated basis. This gives us a maximum energy cap (the energy of the most energetic state in our truncated basis). Using that, we construct a truncated representation of our true H by calculating the matrix elements in the H_0 basis, namely $H_{ij} = \langle i|H|j\rangle$. We can then diagonalize the matrix, finding the low energy values and wavefunctions.

In this project, we will focus on the scalar ϕ^4 theory in (1+1)D (one spatial and temporal dimension each), as it is a simple example of a strongly coupled theory that has hitherto avoided a fully analytical solution [11]. It is the hope that will we will be able to apply this research to more complicated strongly coupled theories (such as QCD) from this jumping-off point. Previous work already exists that attempted to apply Hamiltonian truncation to this theory in the continuum [12]. But ultimately, capping the energy scale on a continuum theory results in UV divergences and non local counter-terms that are hard to avoid.

In response, this work will focus on applying Hamiltonian truncation to a discretized periodic lattice ϕ^4 theory, which sets an energy cutoff of its own due to the lattice spacing. This is due to the fact that the lattice restricts us from probing distances smaller than the spacing, which in turn restricts us from probing the larger energies associated with those short distances. As long as our maximum energy cutoff of the Hilbert space is much greater than the energy scale associated with the lattice spacing, we can hope to avoid the previous problems encountered in the continuum. This method to numerically study ϕ^4 theory has not yet been attempted, so that is what we explore in this project.

Chapter 2

Methodology

Once we have made the transition from the continuum to the lattice, our full ϕ^4 theory Hamiltonian to approximate is

$$H = \sum_x \left[\frac{1}{2}\dot{\hat{\phi}}_x^2 + \frac{(\hat{\phi}_{x+1} - \hat{\phi}_x)^2}{2a^2} + \frac{1}{2}m^2\hat{\phi}_x^2 + \frac{\lambda}{4!}\hat{\phi}_x^4 \right] , \tag{2.1}$$

which is a typical lattice field theory Hamiltonian with a first order finite difference coupling [13]. Here, $\hat{\phi}_x$ is the field operator associated with the lattice site x, a is the lattice spacing, m is the mass of the particles in the associated free theory, and λ is the coupling constant that makes the theory unsolvable when not equal to zero. When λ is large, the field $\hat{\phi}$ is strongly coupled to itself, and the particles in the field interact with each other non-trivially. The sum ranges over L lattice sites.

Our "easy" basis Hamiltonian is

$$H_0 = \sum_x \left[\frac{1}{2}\dot{\hat{\phi}}_x^2 + \frac{1}{2}m^2\hat{\phi}_x^2 \right] . \tag{2.2}$$

We coin this the "ultralocal" Hamiltonian.

Before working on the interacting Hamiltonian (2.1), we will apply our method to the

free Hamiltonian

$$H_{\text{free}} = \sum_x \left[\frac{1}{2}\dot{\hat{\phi}}_x^2 + \frac{(\hat{\phi}_{x+1} - \hat{\phi}_x)^2}{2a^2} + \frac{1}{2}m^2\hat{\phi}_x^2 \right] , \tag{2.3}$$

to compare the approximations the method yields to the exactly solvable quantities available in the non-interacting theory.

One may notice that our choice of H_0 is essentially the same as that of L independent uncoupled harmonic oscillators. This choice is intentional. Because of this, our basis states are simply occupation numbers representing the amount of quanta present in each site: $|\boldsymbol{N}\rangle = |N_1, N_2, ..., N_L\rangle$ (see Figure 1). We use the bold face $\boldsymbol{N}$ to denote the occupation number *vector* with components N_x.

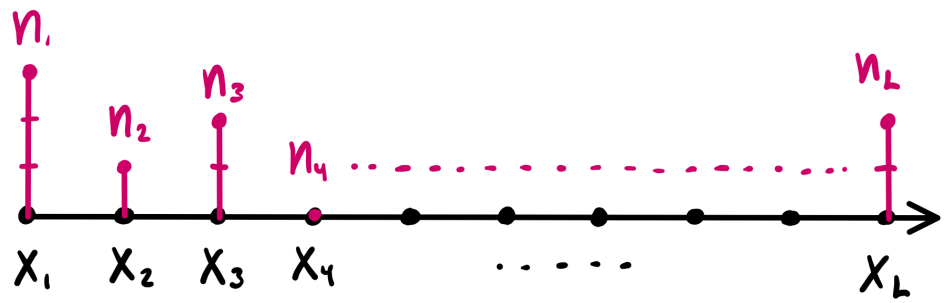

Figure 2.1: Illustration of a typical basis state in the H_0 basis. Each lattice site x has an associated number of quanta, N_x.

We can also express these basis states in terms of creation ($\hat{a}^\dagger$) and annihilation ($\hat{a}$) operators constructed from the ultralocal Hamiltonian. These are defined as follows, and act in analogy with the standard harmonic oscillator algebra:

$$\hat{a}_x^\dagger|\boldsymbol{N}\rangle = \sqrt{N_x+1}|N_1, ..., N_x+1, ..., N_L\rangle \quad \text{and} \quad \hat{a}_x|\boldsymbol{N}\rangle = \sqrt{N_x}|N_1, ..., N_x-1, ..., N_L\rangle \ . \tag{2.4}$$

We can write our H_0 basis states in terms of these operators by defining new operators $\hat{A}(\boldsymbol{N})$ and $\hat{A}^\dagger(\boldsymbol{N})$:

$$\hat{A}(\boldsymbol{N}) = \prod_x \frac{\hat{a}_x^{N_x}}{\sqrt{N_x!}} \quad \text{and} \quad \hat{A}^\dagger(\boldsymbol{N}) = \prod_x \frac{(\hat{a}_x^\dagger)^{N_x}}{\sqrt{N_x!}} \tag{2.5}$$

which destroy and create the states $|\boldsymbol{N}\rangle$ respectively, i.e. $\hat{A}^\dagger(\boldsymbol{N})|0\rangle = |\boldsymbol{N}\rangle$. If we choose the vacuum $|0\rangle$ to be normalized to one, then these basis states are also normalized to one:

$$\langle \boldsymbol{N}|\boldsymbol{N}\rangle = \langle 0|\hat{A}(\boldsymbol{N})\hat{A}^\dagger(\boldsymbol{N})|0\rangle = 1 \tag{2.6}$$

This information is enough to construct the matrix elements $\langle \boldsymbol{N'}|H|\boldsymbol{N}\rangle$. After doing so, we will be able to diagonalize the matrix and calculate the eigenvalues, eigenstates, and therefore other observables and expectation values.

2.1 Calculating the Matrix Elements

To actually compute these elements, we must introduce some more formalism to simplify the problem. To make the computational process significantly more efficient, we will restrict ourselves to the subspace of translationally invariant states on the lattice. Physically, this means we only consider states consisting of pairs of particles with equal and opposite momenta. Most notably, the ground state is included in this subspace. We can construct such a translationally invariant state out of any occupation number vector $\boldsymbol{N}$ by summing all lattice translations of the state that occupation number represents. Mathematically, our translationally invariant state $|\bar{\boldsymbol{N}}\rangle$ will be:

$$|\bar{\boldsymbol{N}}\rangle \propto \sum_\xi |\boldsymbol{N}_\xi\rangle = \sum_\xi \hat{A}^\dagger(\boldsymbol{N}_\xi)|0\rangle \tag{2.7}$$

where we sum over all possible translations ξ on the lattice, meaning $(\boldsymbol{N_\xi})_x = N_{x+\xi}$. We can also express these states in terms of a translation operator T_ξ so that:

$$|\bar{\boldsymbol{N}}\rangle \propto \sum_\xi \hat{T}_\xi \hat{A}^\dagger(\boldsymbol{N})|0\rangle \ , \quad \text{where} \quad \hat{T}_\xi \hat{A}^\dagger(\boldsymbol{N}) = \hat{A}^\dagger(\boldsymbol{N}_\xi) \ . \tag{2.8}$$

The normalization of these states depends on the 'symmetry factor' of $\boldsymbol{N}$, which we

denote $S_{\boldsymbol{N}}$. This factor is simply the number of translations ξ that result in the same original occupation number vector. With this convention, our normalization is:

$$|\bar{\boldsymbol{N}}\rangle = \frac{1}{\sqrt{S_{\boldsymbol{N}} L}} \sum_{\xi} \hat{T}_{\xi} \hat{A}^{\dagger}(\boldsymbol{N})|0\rangle \ . \tag{2.9}$$

To make use of this formalism in calculating the desired matrix elements, we must write the Hamiltonian H completely in terms of the creation and annihilation operators $\hat{a}_x$ and $\hat{a}_x^{\dagger}$. This is done through the standard relations

$$\hat{\phi}_x = \frac{1}{\sqrt{2m}}(\hat{a}_x + \hat{a}_x^{\dagger}) \quad \text{and} \quad \hat{\dot{\phi}}_x = -i\sqrt{\frac{m}{2}}(\hat{a}_x - \hat{a}_x^{\dagger}) \tag{2.10}$$

and through normal ordering, ensuring each term in the Hamiltonian is arranged so all creation operators are on the left, and all annihilation operators are on the right (see Appendix A). Completing this process, the free lattice Hamiltonian becomes:

$$\begin{aligned} H_{\text{free}} = \sum_{x}^{L} m(\hat{a}_x^{\dagger}\hat{a}_x + \frac{1}{2}) + \sum_{x}^{L} \frac{1}{2ma^2} \Big[&(\hat{a}_x^2 + \text{h.c.}) - (\hat{a}_x \hat{a}_{x+1} + \text{h.c.}) \\ &- (\hat{a}_{x+1}^{\dagger}\hat{a}_x + \text{h.c.}) + 2\hat{a}_x^{\dagger}\hat{a}_x + 1 \Big] \end{aligned} \tag{2.11}$$

and the interacting Hamiltonian is:

$$\begin{aligned} H = \sum_{x}^{L} m(\hat{a}_x^{\dagger}\hat{a}_x + \frac{1}{2}) + \sum_{x}^{L} \Bigg[&\frac{\lambda}{96m^2}(\hat{a}_x^4 + \text{h.c.}) + \frac{8+\lambda a^2}{16ma^2}(\hat{a}_x^2 + \text{h.c.}) \\ &+ \frac{\lambda}{24m^2}(\hat{a}_x^{\dagger}\hat{a}_x^3 + \text{h.c.}) - \frac{1}{2m}\left[(\hat{a}_x\hat{a}_{x+1} + \text{h.c.}) + (\hat{a}_{x+1}^{\dagger}\hat{a}_x + \text{h.c.})\right] \\ &+ \frac{\lambda}{16m^2}(\hat{a}_x^{\dagger})^2(\hat{a}_x)^2 - \frac{8+\lambda a^2}{8ma^2}\hat{a}_x^{\dagger}\hat{a}_x + \frac{16+\lambda a^2}{32ma^2} \Bigg] \ . \end{aligned} \tag{2.12}$$

What we have effectively done is put the Hamiltonians into the form of a linear combi-

nation of all normal ordered operators, or:

$$H = \sum_{\boldsymbol{n}',\boldsymbol{n}} h_{\boldsymbol{n}',\boldsymbol{n}} \mathcal{O}(\boldsymbol{n}',\boldsymbol{n}) \ , \quad \text{where} \quad \mathcal{O}(\boldsymbol{n}',\boldsymbol{n}) = \prod_x (\hat{a}_x^\dagger)^{n'_x} (\hat{a}_x)^{n_x} \tag{2.13}$$

where $\boldsymbol{n}', \boldsymbol{n}$ are occupation number vectors. The problem of finding $\langle \bar{\boldsymbol{N}}' | H | \bar{\boldsymbol{N}} \rangle$ is then reduced to finding the elements $\langle \bar{\boldsymbol{N}}' | \mathcal{O}(\boldsymbol{n}',\boldsymbol{n}) | \bar{\boldsymbol{N}} \rangle$ for any given $\boldsymbol{n}', \boldsymbol{n}$. The full calculation of this general quantity can be found in Appendix B, but here we will state the answer in the most computationally helpful form:

$$\begin{aligned} \langle \bar{\boldsymbol{N}}' | \mathcal{O}(\boldsymbol{n}',\boldsymbol{n}) | \bar{\boldsymbol{N}} \rangle = \frac{\sqrt{S_{\boldsymbol{N}'} S_{\boldsymbol{N}}}}{L} \prod_x \sqrt{\frac{(T_\gamma N'_x - n'_x + n_x)!}{(T_\gamma N'_x - n'_x)!} \frac{(T_\gamma N'_x)!}{(T_\gamma N'_x - n'_x)!}} \\ \times \theta(T_\gamma N'_x - n'_x) \delta_{(T_\gamma N'_x - n'_x),(T_\sigma N_x - n_x)} \end{aligned} \tag{2.14}$$

The notation for this formula is somewhat non-standard, but it can be understood in terms of the theta and delta functions in front. The Kronecker delta tells us to first check if there exists a γ and σ such that the occupation number vectors $T_\gamma \boldsymbol{N}' - \boldsymbol{n}'$ and $T_\sigma \boldsymbol{N} - \boldsymbol{n}$ are equal. If there are no such γ and σ, the matrix element is zero. The theta function then tells us that the matrix element is non-zero still only if the vector $T_\gamma \boldsymbol{N}' - \boldsymbol{n}'$ is greater than or equal to 0 at each lattice site. If it is, then we plug the shift γ into the remaining part of the formula and compute the matrix element.

This expression is helpful because it allows us an efficient method to check whether a given matrix element will be zero, which will be the case the vast majority of the time. We now have most of the pieces we need; given a basis for H_0 ($\{|\bar{\boldsymbol{N}}\rangle\}$), we can compute the matrix elements of H in this basis in terms of its normal ordered operators.

2.2 Generating the Basis

But how do we generate our computational basis $\{|\bar{\boldsymbol{N}}\rangle\}$? This approximation method will only be viable if our basis is quite large, so how do we create it? There are numerous ways

to generate random basis states of H_0, but our chosen method was to repeatedly act the Hamiltonian H on the ground state of H_0:

$$\{|\boldsymbol{N}\rangle\} = \{H^n|0\rangle \;||\; n \in \mathbb{N}\} \; . \tag{2.15}$$

Since the Hamiltonian is a linear combination of normal ordered operators of the form $\mathcal{O} = \prod(\hat{a}_x^\dagger)^{n\prime}(\hat{a}_x)^{n\prime}$, then it is clear that operators like $\hat{a}_{x+1}^\dagger \hat{a}_x$ or $\hat{a}_x^\dagger$ will produce new basis states. In fact, these operators that create off-diagonal matrix elements of H are the only ones we need to consider in creating our H_0 basis. In other words, given the division $H = H_0 + V$, we can rewrite our generated basis as

$$\{|\boldsymbol{N}\rangle\} = \{V^n|0\rangle \;||\; n \in \mathbb{N}\} \; , \tag{2.16}$$

since the action of H_0 on a state $|\boldsymbol{N}\rangle$ will not produce any new occupation number vectors. Of course, this simply gets us a list of occupation number vectors, which we must then turn into translationally invariant states so we can apply our formulas above.

There are qualitative reasons that support choosing this particular method of basis generation, since it is related to projecting random states in the Hilbert space onto the ground state. For example, we can make such a projection by evolving any state through imaginary time τ. Let $\{|n\rangle\}$ be the eigenbasis for H. For any $|\boldsymbol{N}\rangle$ in the H_0 basis, we then have:

$$e^{-H\tau}|\boldsymbol{N}\rangle = e^{-H\tau}\sum_n c_n|n\rangle = \sum_n e^{-E_n\tau}c_n|n\rangle \; , \tag{2.17}$$

and we can see that as $\tau \to \infty$, the state $|N\rangle$ is projected onto the ground state, where E_n is minimized. But we can also rewrite this projection as:

$$e^{-H\tau}|\boldsymbol{N}\rangle = \sum_m \frac{(-H\tau)^m}{m!}|\boldsymbol{N}\rangle \; . \tag{2.18}$$

So by adding the states $H^m|\boldsymbol{N}\rangle$ to our basis, we are potentially creating the necessary states to achieve the projection onto the ground state.

With all this formalism, we then created a program that automates this process: generating a truncated basis, calculating the matrix elements of H within that basis, then diagonalizing that representation of H to find the eigenstates and eigenvalues. This program was written in the Julia languange.

Chapter 3

Results and Discussion

3.1 General Convergence Results

3.1.1 Free Theory Convergence

Before we attempt to use this method on ϕ^4 theory, we will first apply it to free theory on the lattice to test its validity. Our method will still "approximate" the free theory because we are still using a finite-dimensional basis to approximately span the infinite dimensional Hilbert space. However, it is useful to test on free theory because we can calculate the error between our approximation and the true values we wish to approximate. Our residual error we measure will simply be a percent-error, meaning:

$$\text{Residual} = \frac{\text{Numerical} - \text{Theoretical}}{\text{Theoretical}} \ . \tag{3.1}$$

We will use the lowest two (translationally invariant) state energies as well as the $\langle \hat{\phi}^2 \rangle$ vacuum expectation value to quantitatively test the convergence. The lowest energy state will be the ground state (vacuum), and the second lowest energy state will be the state with two particles going in opposite directions, each with the lowest non-zero momentum possible.

We can see from figure 3.1 that the estimates are certainly converging to their theoretical

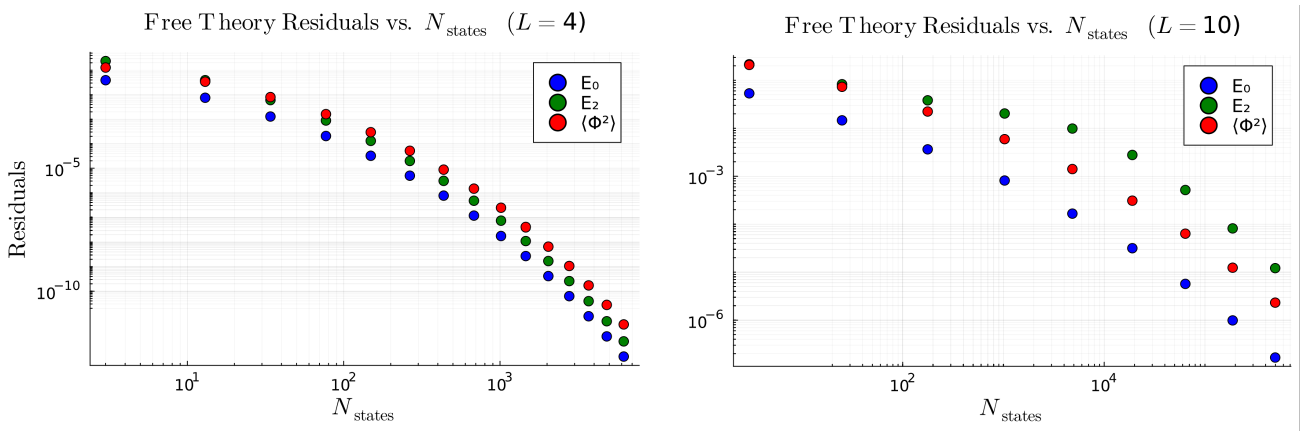

Figure 3.1: Log log plots of the residuals of our three test quantities of interest: the lowest two energy states on the $L = 4, 10$ lattices, as well as the vacuum expectation value of $\langle\hat{\phi}^2\rangle$, versus the number of states in our computational basis N_{states}.

values, but this convergence becomes slower as the lattice size increases. Even more explicitly, figure 3.2 shows the direct comparison of estimates for different lattice sizes, and how as the lattice size increases, the convergence rate becomes drastically slower. The largest lattice in this plot is $L = 10$, which is not at all large in the realm of lattice field theory simulations. We can interpolate from this plot that as we keep increasing the lattice size, the slope of the log residual data will become almost horizontal, rendering this method effectively useless.

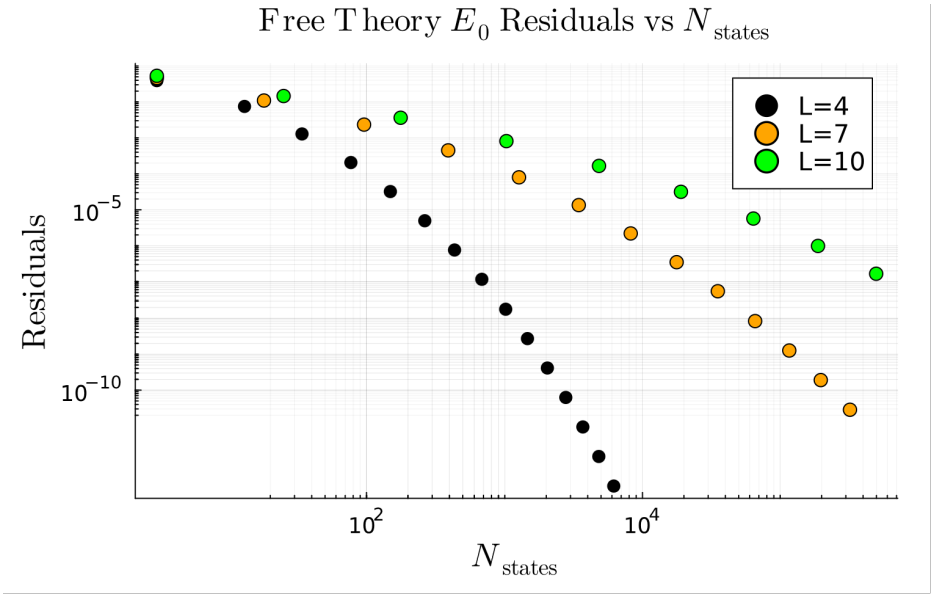

Figure 3.2: Log-log plot of the free theory vacuum energy residuals on the $L = 4, 7, 10$ lattices vs N_{states}.

3.1.2 ϕ^4 Theory Convergence

Once we move to ϕ^4 theory, the story does not meaningfully change. We can no longer exactly calculate the residual error, so we instead use a crude estimation. We simply assert that the jump in accuracy with each increase of N_{states} is approximately equal to the total error before the increase. In other words, if E_N is an energy estimate given N states in the computational basis, $E_{N'}$ is a better estimate where $N' \gg N$, and ΔE_N is the actual error of the first estimate, then we assert:

$$\Delta E_N \approx E_N - E_{N'} \ . \tag{3.2}$$

Using this assertion to calculate the residual ground state errors in the same manner as the free theory case, figure 3.3 illustrates the results for the same three lattice sizes. For this plot, we picked the coupling parameter λ to be in the non-perturbative regime, specifically $\lambda/m^2 = 3$. The same qualitative trend holds; the convergence rate decreases rapidly as lattice size increases.

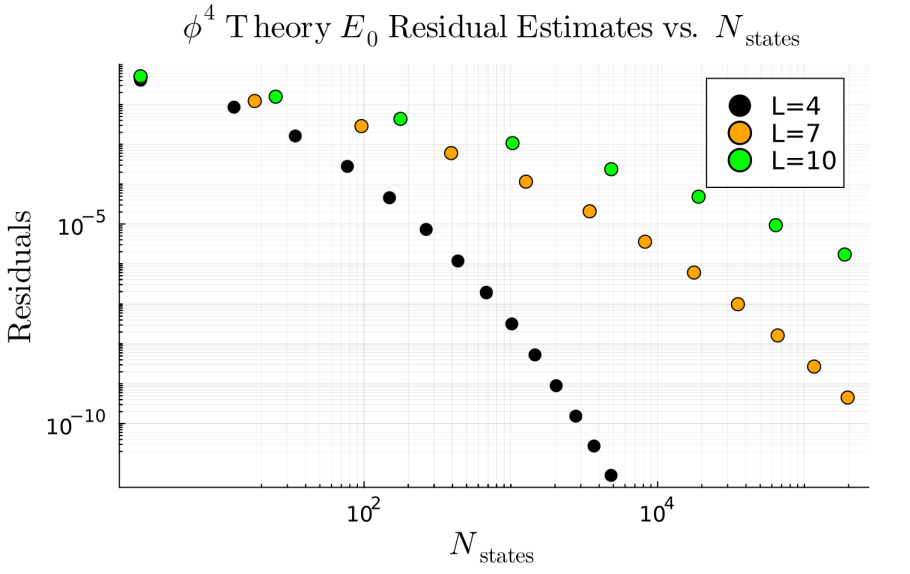

Figure 3.3: Log-log plot of the ϕ^4 theory ($\lambda/m^2 = 3$) ground state energy residual estimates vs N_{states}, comparing different lattice sizes $L = 4, 7, 10$.

3.2 Critical Coupling

The previous results seem damning, but there is still a possibility for interesting results to be made with this method. In particular, we can use the Binder cumulant, named after Austrian physicist Kurt Binder, to estimate the value of the critical coupling $\frac{m^2}{\lambda}$ of ϕ^4 theory. The Binder cumulant is useful for identifying critical points of phase transitions [14, 15], thus also useful for studying ϕ^4 theory as it exhibits such a phase transition when the coupling (λ) of the theory reaches a certain critical value relative to the mass parameter of the theory (m^2) [16]. This is due to spontaneous symmetry breaking in the ground state in the infinite volume limit.

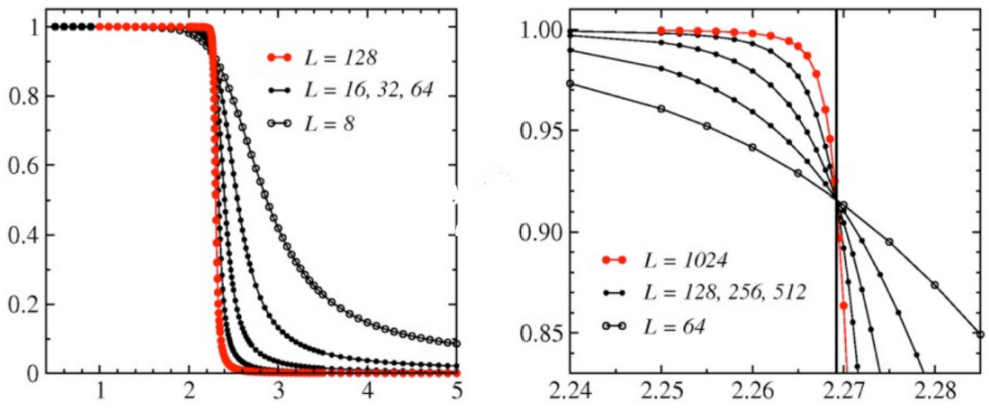

Figure 3.4: Example plots of a typical use of a Binder cumulant. The cumulant is graphed across a specific parameter of the theory for many different lattice sizes, and all lattice curves intersect at the same point [1].

The Binder cumulant U_L is defined (in this context) as:

$$U_L\left(\frac{m^2}{\lambda}\right) = 1 - \frac{1}{3}\frac{\langle\hat{\bar{\phi}}^4\rangle_L}{\langle\hat{\bar{\phi}}^2\rangle_L^2}\ , \tag{3.3}$$

where it is dependent on two variables, the lattice size L, and the dimensionless coupling of the theory m^2/λ. The expectation values are taken with respect to the vacuum. The operator $\hat{\bar{\phi}}$ is defined as the average of the field operators $\hat{\phi}_x$ over the lattice. Since the lattice itself is isotropic, we trivially have $\hat{\bar{\phi}} = \hat{\phi}_x$ for all lattice sites. However, when the

averaged field operator is raised to a power it is not so simple, for example:

$$\begin{aligned}\hat{\bar{\phi}}^2 &= \left(\frac{1}{L}\sum_x \hat{\phi}_x\right)^2 = \frac{1}{L^2}\left[\sum_x \frac{1}{\sqrt{2m}}\left(\hat{a}_x^\dagger + \hat{a}_x\right)\right]^2 \\ &= \frac{1}{2mL^2}\left[\left(\sum_{x,x'} \hat{a}_x^\dagger \hat{a}_{x'}^\dagger + \hat{a}_x \hat{a}_{x'} + 2\hat{a}_x^\dagger \hat{a}_{x'}\right) + L\right] \quad .\end{aligned} \tag{3.4}$$

We can calculate the matrix elements, and therefore expectation values, of these operators with the methods described above.

The Binder cumulant works as follows. We wish to determine the value of the dimensionless coupling m^2/λ at which the phase transition occurs in the infinite volume limit. If we were to plot U_∞ against this coupling, we would see it take two different values on either side of the critical value input, instantaneously switching between the two at the critical point. We cannot plot this curve as we cannot simulate an infinite lattice. However, we can plot the curves for various finite lattice sizes, U_L. Intuitively, these curves should approach U_∞ as $L \to \infty$.

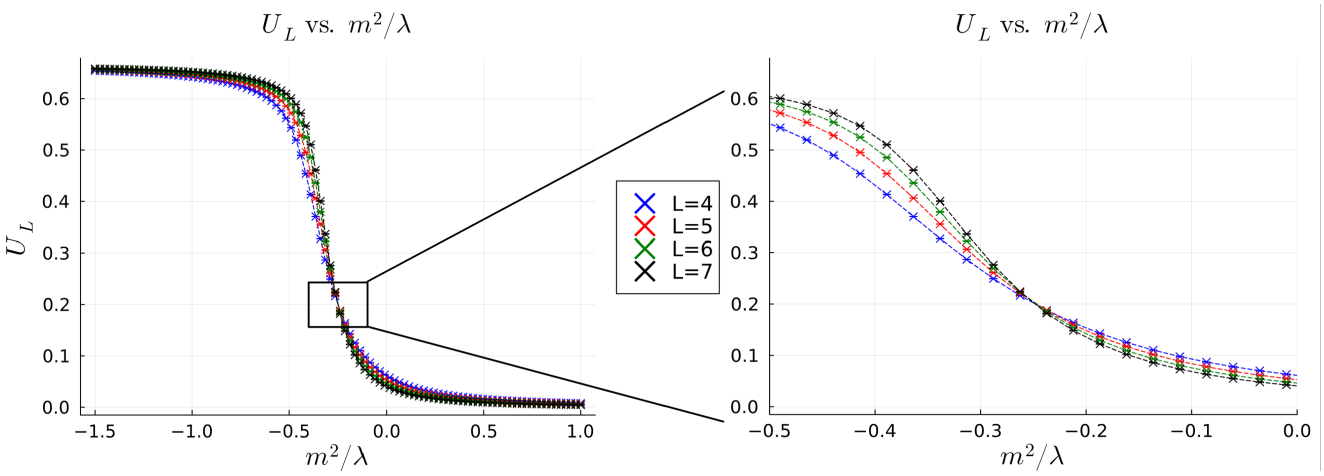

Figure 3.5: My Binder cumulant plots for ϕ^4 theory on the lattice. We plot the cumulant against the value of $\frac{\lambda}{m^2}$ for 4 different lattice sizes, and see that they have a common intersection point (~ -0.25).

Furthermore, as Kurt Binder worked out [14], all of the finite L curves must intersect at a common point. Figure 3.4 illustrates an example of this process for a similar measurement

in condensed matter physics [1]. Because the curves for all lattice sizes must intersect at a common point, this common point *must* be the value of the critical point at which the phase transition occurs.

This is the procedure that we replicate. In figure 3.5, we plot U_L for $L = 4, 5, 6, 7$, and find their common intersection point. We find the value of the dimensionless coupling at this intersection is approximately $m^2/\lambda \approx -0.25$. This measurement agrees with [17], where the same measurement of the dimensionless critical coupling of (1+1)d ϕ^4 theory was made through different means.

This shows that despite the potentially discouraging convergence rates for this implementation of Hamiltonian truncation, there are still possibilities for interesting measurements to be made.

Chapter 4

Conclusions

4.1 Lattice Hamiltonian Truncation: Yay or Nay?

Overall, the interest in this specific project was exploratory. As far as we know, this particular implementation of Hamiltonian truncation has not yet been attempted, so the goal of this project was to see how it fared against other implementations, as well as entirely different methods that accomplish the same task.

Comparing against other implementations of Hamiltonian truncation, we are able to simulate lattices of greater volumes. The traditional approach of Hamiltonian truncation does not take place on the lattice, but on the continuum, where the Hilbert space is truncated with a simple cap on momentum eigenstates of the free continuum theory [12, 18, 19, 20, 21]. In our implementation, the lattice acts as one "cutoff", but we also truncate the Hilbert space in a less trivial way, by creating a computational basis with the ultralocal Hamiltonian and only using states therein. Ultimately, our method leads to greater potential lattice sizes and accuracy with comparable computational resources to the traditional methods.

However, both methods suffer heavily from volume scaling issues. Whether we are in the continuum or on the lattice, the computational cost is exponential in the size of the lattice. This is qualitatively demonstrated in the lattice method from figures 3.2 and 3.3.

As the lattice size increases, we need exponentially more basis states to achieve reasonable accuracy. This is very bad news, since our original goal was to analyze low energy behavior of strongly coupled theories, like QCD. The way we study this low energy behavior is to calculate long-distance correlation functions (how stuff over here affects stuff over there), and since those correlation lengths cannot be larger than the volume, we find an exponential barrier directly in the way of our goal. The best we can do is to use the changing volume as a probe of the system, as we have done with the Binder cumulant to estimate the critical coupling. So it seems that Hamiltonian truncation is still not suited to the needs of studying strong coupling.

For further comparison and reference, alternative methods of analyzing strongly coupled theories and the long-distance correlations therein are more successful at overcoming this barrier. The state-of-the-art method most commonly used to study such theories is called matrix product states, or tensor network states [22, 23, 24]. In these computational methods, the computational complexity scales only with the *area* (or perimeter) of the lattice, not the volume. This drastically increases the efficiency and accuracy compared to Hamiltonian truncation. In fact, if the lattice only occupies one spatial dimension, then the computational complexity is not dependent on the size of the lattice, since the perimeter (the endpoints) does not change! This is a stark difference from the method tried in this paper, and is clearly the more efficient choice.

Chapter 5

Acknowledgments

I would like to thank the NSF REU Program and UC Davis for sponsoring this opportunity for myself and my peers. In particular, I would like to thank Dr. Markus Luty, Ben Eustace-Guthrie, and Pavel Press for making this research experience an absolute pleasure.

Chapter 6

References

[1] T. Mendes-Santos, A. Angelone, A. Rodriguez, R. Fazio, and M. Dalmonte, "Intrinsic dimension of path integrals: Data-mining quantum criticality and emergent simplicity," *PRX Quantum*, vol. 2, aug 2021.

[2] T. Aoyama, M. Hayakawa, T. Kinoshita, and M. Nio, "Tenth-order QED contribution to the electron g-2 and an improved value of the fine structure constant," *Physical Review Letters*, vol. 109, sep 2012.

[3] M. E. Peskin and D. V. Schroeder, *An Introduction to Quantum Field Theory*. Westview Press, 1995. Reading, USA: Addison-Wesley (1995) 842 p.

[4] R. P. Feynman, "Space-time approach to quantum electrodynamics," *Physical Review*, vol. 76, pp. 769–789, sep 1949.

[5] J. Schwinger, "Quantum electrodynamics. i. a covariant formulation," *Physical Review*, vol. 74, pp. 1439–1461, nov 1948.

[6] F. Wilczek, "Nobel lecture: Asymptotic freedom: From paradox to paradigm," *Reviews of Modern Physics*, vol. 77, pp. 857–870, sep 2005.

[7] C. Ratti, "Lattice QCD and heavy ion collisions: a review of recent progress," *Reports on Progress in Physics*, vol. 81, p. 084301, jul 2018.

[8] A. Milsted, J. Haegeman, and T. J. Osborne, "Matrix product states and variational methods applied to critical quantum field theory," *Physical Review D*, vol. 88, oct 2013.

[9] L. Funcke, K. Jansen, and S. Kuhn, "Topological vacuum structure of the schwinger model with matrix product states," *Physical Review D*, vol. 101, mar 2020.

[10] B. Buyens, J. Haegeman, K. V. Acoleyen, H. Verschelde, and F. Verstraete, "Matrix product states for gauge field theories," *Physical Review Letters*, vol. 113, aug 2014.

[11] G. Gallavotti and V. Rivasseau, "ϕ^4 field theory in dimension 4 : a modern introduction to its unsolved problems," *Annales de l'I.H.P. Physique théorique*, vol. 40, no. 2, pp. 185–220.

[12] T. Cohen, K. Farnsworth, R. Houtz, and M. Luty, "Hamiltonian truncation effective theory," *SciPost Physics*, vol. 13, aug 2022.

[13] J. Smit, *Introduction to Quantum Fields on a Lattice*. Cambridge Lecture Notes in Physics, Cambridge University Press, 2002.

[14] K. Binder, "Critical properties from monte carlo coarse graining and renormalization," *Phys. Rev. Lett.*, vol. 47, pp. 693–696, Aug 1981.

[15] "Binder cumulants and phase transitions." `http://www.lptms.u-psud.fr/membres/trizac/Ens/PCS/TD1_Binder.pdf`, 2023. Accessed: 2023-10-30.

[16] J. F. Yang, "Dynamical symmetry breaking of massless $\lambda\phi^4$ and renormalization scheme dependence," 2001.

[17] A. K. De, A. Harindranath, J. Maiti, and T. Sinha, "Investigations in $1+1$ dimensional lattice ϕ^4 theory," *Phys. Rev. D*, vol. 72, p. 094503, Nov 2005.

[18] M. Hogervorst, S. Rychkov, and B. C. van Rees, "Truncated conformal space approach in d dimensions: A cheap alternative to lattice field theory?," *Phys. Rev. D*, vol. 91, p. 025005, Jan 2015.

[19] S. Rychkov and L. G. Vitale, "Hamiltonian truncation study of the φ^4 theory in two dimensions," *Phys. Rev. D*, vol. 91, p. 085011, Apr 2015.

[20] S. Rychkov and L. G. Vitale, "Hamiltonian truncation study of the ϕ^4 theory in two dimensions. ii. the $\mathbb{Z}_2$-broken phase and the chang duality," *Phys. Rev. D*, vol. 93, p. 065014, Mar 2016.

[21] J. Elias-Miró, S. Rychkov, and L. G. Vitale, "Nlo renormalization in the hamiltonian truncation," *Phys. Rev. D*, vol. 96, p. 065024, Sep 2017.

[22] J. I. Cirac, D. Pérez-García, N. Schuch, and F. Verstraete, "Matrix product states and projected entangled pair states: Concepts, symmetries, theorems," *Rev. Mod. Phys.*, vol. 93, p. 045003, Dec 2021.

[23] R. Orús, "A practical introduction to tensor networks: Matrix product states and projected entangled pair states," *Annals of Physics*, vol. 349, pp. 117–158, 2014.

[24] B. Buyens, J. Haegeman, K. Van Acoleyen, H. Verschelde, and F. Verstraete, "Matrix product states for gauge field theories," *Phys. Rev. Lett.*, vol. 113, p. 091601, Aug 2014.

Appendix A

Normal Ordered Hamiltonian

Here we describe how to "normal order" the Hamiltonian in terms of the creation and annihilation operators present in each operator composing it. Normal ordering simply means rewriting each observable present in the Hamiltonian in terms of the ultralocal creation and annihilation operators using the relations

$$\hat{\phi}_x = \frac{1}{\sqrt{2m}}(\hat{a}_x^\dagger + \hat{a}_x) \quad \text{and} \quad \dot{\hat{\phi}}_x = i\sqrt{\frac{m}{2}}(\hat{a}_x^\dagger - \hat{a}_x) \ , \tag{A.1}$$

and then using the commutator of the creation and annihilation operators:

$$\left[\hat{a}_x, \hat{a}_y^\dagger\right] = \delta_{xy} \ , \tag{A.2}$$

to put all of the creation operators on the left of the annihilation operators. The free lattice Hamiltonian is:

$$H_{\text{free}} = \sum_x \left[\frac{1}{2}\dot{\hat{\phi}}_x^2 + \frac{(\hat{\phi}_{x+1} - \hat{\phi}_x)^2}{2a^2} + \frac{1}{2}m^2\hat{\phi}_x^2\right] \ . \tag{A.3}$$

To normal order this, we first expand each operator within in terms of the creation and annihilation operators. We begin with $\hat{\phi}_x^2$:

$$\begin{aligned}\hat{\phi}_x^2 &= \frac{1}{2m}(\hat{a}_x^\dagger + \hat{a}_x)^2 \\ &= \frac{1}{2m}\left((\hat{a}_x^\dagger)^2 + (\hat{a}_x)^2 + \hat{a}_x^\dagger\hat{a}_x + \hat{a}_x\hat{a}_x^\dagger\right) \\ &= \frac{1}{2m}\left((\hat{a}_x^\dagger)^2 + (\hat{a}_x)^2 + 2\hat{a}_x^\dagger\hat{a}_x + 1\right) \ ,\end{aligned} \tag{A.4}$$

where we used the commutator in the last step. Similarly, for the conjugate momentum we have:

$$\dot{\hat{\phi}}_x^2 = -\frac{m}{2}\left((\hat{a}_x^\dagger)^2 + (\hat{a}_x)^2 - 2\hat{a}_x^\dagger\hat{a}_x - 1\right) \ . \tag{A.5}$$

Now we tackle the derivative term. We have:

$$\left(\hat{\phi}_x - \hat{\phi}_{x+1}\right)^2 = \hat{\phi}_x^2 + \hat{\phi}_{x+1}^2 - 2\hat{\phi}_x\hat{\phi}_{x+1} \ , \tag{A.6}$$

since operators on different lattice sites commute. We already have expressions for the first two terms, and we can calculate the final term with:

$$\begin{aligned}\hat{\phi}_x\hat{\phi}_{x+1} &= \frac{1}{2m}(\hat{a}_x^\dagger + \hat{a}_x)(\hat{a}_{x+1}^\dagger + \hat{a}_{x+1}) \\ &= \frac{1}{2m}\left(\hat{a}_x^\dagger\hat{a}_{x+1}^\dagger + \hat{a}_x^\dagger\hat{a}_{x+1} + \hat{a}_{x+1}^\dagger\hat{a}_x + \hat{a}_x\hat{a}_{x+1}\right) \ .\end{aligned} \tag{A.7}$$

So our finite difference derivative term is then:

$$\begin{aligned}\left(\hat{\phi}_x - \hat{\phi}_{x+1}\right)^2 &= \frac{1}{2m}\left((\hat{a}_x^\dagger)^2 + (\hat{a}_x)^2 + 2\hat{a}_x^\dagger\hat{a}_x + 1\right) \\ &\quad + \frac{1}{2m}\left((\hat{a}_{x+1}^\dagger)^2 + (\hat{a}_{x+1})^2 + 2\hat{a}_{x+1}^\dagger\hat{a}_{x+1} + 1\right) \\ &\quad - \frac{1}{m}\left(\hat{a}_x^\dagger\hat{a}_{x+1}^\dagger + \hat{a}_x^\dagger\hat{a}_{x+1} + \hat{a}_{x+1}^\dagger\hat{a}_x + \hat{a}_x\hat{a}_{x+1}\right) \ .\end{aligned} \tag{A.8}$$

Putting this all together into our Hamiltonian, and simplifying, we obtain:

$$H_{\text{free}} = \sum_{x}^{L} m(\hat{a}_x^\dagger \hat{a}_x + \frac{1}{2}) + \sum_{x}^{L} \frac{1}{2ma^2} \Big[(\hat{a}_x^2 + \text{h.c.}) - (\hat{a}_x \hat{a}_{x+1} + \text{h.c.}) \\ - (\hat{a}_{x+1}^\dagger \hat{a}_x + \text{h.c.}) + 2\hat{a}_x^\dagger \hat{a}_x + 1 \Big] . \tag{A.9}$$

The same exact techniques can be applied to the $\hat{\phi}_x^4$ operator to compute the normal ordered Hamiltonian for ϕ^4 theory.

Appendix B

Calculation of Matrix Elements

In this section we calculate the matrix elements $\langle \bar{\boldsymbol{N}}' | \mathcal{O}(\boldsymbol{n}', \boldsymbol{n}) | \bar{\boldsymbol{N}} \rangle$ for any given normal ordered operator $\mathcal{O}(\boldsymbol{n}', \boldsymbol{n})$. Expanding this out in terms of our previous definitions, we have:

$$\langle \bar{\boldsymbol{N}}' | \mathcal{O}(\boldsymbol{n}', \boldsymbol{n}) | \bar{\boldsymbol{N}} \rangle = \frac{1}{L\sqrt{S_{N'} S_N}} \sum_{\xi'} \sum_{\xi} \langle 0 | \hat{A}_{N'} \hat{T}_{\xi'} \mathcal{O}(\boldsymbol{n}', \boldsymbol{n}) \hat{T}_{\xi} \hat{A}_N^\dagger | 0 \rangle \ . \tag{B.1}$$

Let us focus on just the latter portion, expanding the normal ordered operator $\mathcal{O}$:

$$\begin{aligned} \mathcal{O}(\boldsymbol{n}', \boldsymbol{n}) \hat{T}_{\xi} \hat{A}_N^\dagger | 0 \rangle &= \prod_x (\hat{a}_x^\dagger)^{n'_x} (\hat{a}_x)^{n_x} \frac{(\hat{a}_{x+\xi}^\dagger)^{N_x}}{\sqrt{N_x!}} | 0 \rangle \\ &= \prod_x (\hat{a}_x^\dagger)^{n'_x} (\hat{a}_x)^{n_x} \frac{(\hat{a}_x^\dagger)^{N_{x-\xi}}}{\sqrt{N_{x-\xi}!}} | 0 \rangle \ . \end{aligned} \tag{B.2}$$

Because annihilation operators send the vacuum to 0, then if $n_x > N_{x-\xi}$, this expression will be 0. Therefore, we assume otherwise, but add a step function to account for the possibility.

In particular,

$$
\begin{aligned}
(\hat{a}_x)^{n_x}\frac{(\hat{a}_x^\dagger)^{N_{x-\xi}}}{\sqrt{N_{x-\xi}!}}|0\rangle &= (\hat{a}_x)^{n_x}|N_{x-\xi}\rangle \\
&= \theta(N_{x-\xi}-n_x)\frac{\sqrt{N_{x-\xi}!}}{\sqrt{(N_{x-\xi}-n_x)!}}|N_{x-\xi}-n_x\rangle \\
&= \theta(N_{x-\xi}-n_x)\frac{\sqrt{N_{x-\xi}!}}{(N_{x-\xi}-n_x)!}(\hat{a}_x^\dagger)^{N_{x-\xi}-n_x}|0\rangle \ .
\end{aligned} \tag{B.3}
$$

Inserting this back in to B.2, we have:

$$
\mathcal{O}(\boldsymbol{n}',\boldsymbol{n})\hat{T}_\xi\hat{A}_N^\dagger|0\rangle = \prod_x \theta(N_{x-\xi}-n_x)\frac{\sqrt{N_{x-\xi}!}}{(N_{x-\xi}-n_x)!}(\hat{a}_x^\dagger)^{N_{x-\xi}-n_x+n'_x}|0\rangle \ . \tag{B.4}
$$

Then, from our definition of $\hat{A}_N^\dagger$, we have

$$
\hat{A}^\dagger_{T_\xi N-n+n'} = \prod_x \frac{(\hat{a}_x^\dagger)^{N_{x-\xi}-n_x+n'_x}}{\sqrt{(N_{x-\xi}-n_x+n'_x)!}} \ , \tag{B.5}
$$

and therefore

$$
\left(\prod_x \sqrt{(N_{x-\xi}-n_x+n'_x)!}\right)\hat{A}^\dagger_{T_\xi N-n+n'} = \prod_x (\hat{a}_x^\dagger)^{N_{x-\xi}-n_x+n'_x} \ . \tag{B.6}
$$

Inserting this into B.4 yields:

$$
\mathcal{O}(\boldsymbol{n}',\boldsymbol{n})\hat{T}_\xi\hat{A}_N^\dagger|0\rangle = \left[\prod_x \theta(N_{x-\xi}-n_x)\sqrt{\frac{N_{x-\xi}!\ (N_{x-\xi}-n_x+n'_x)!}{(N_{x-\xi}-n_x)!\ (N_{x-\xi}-n_x)!}}\right]\hat{A}^\dagger_{T_\xi N-n+n'}|0\rangle \ . \tag{B.7}
$$

We can now plug this back into our original expression in B.1 to get

$$
\begin{aligned}
\langle\bar{\boldsymbol{N}}'|\mathcal{O}(\boldsymbol{n}',\boldsymbol{n})|\bar{\boldsymbol{N}}\rangle = \frac{1}{L\sqrt{S_{N'}S_N}}\sum_\xi &\left[\prod_x \theta(N_{x-\xi}-n_x)\sqrt{\frac{N_{x-\xi}!\ (N_{x-\xi}-n_x+n'_x)!}{(N_{x-\xi}-n_x)!\ (N_{x-\xi}-n_x)!}}\right] \\
&\times\sum_{\xi'}\langle 0|\hat{A}_{N'}\hat{T}_{\xi'}\hat{A}^\dagger_{T_\xi N-n+n'}|0\rangle \ .
\end{aligned} \tag{B.8}
$$

We now evaluate the bottom sum, considering ξ to be fixed. If a term in the sum is non-zero, it means that $\hat{T}_{\xi'}N' = \hat{T}_{\xi}N - n + n'$, in which case that term will be exactly 1 from the vacuum normalization. However, if this is true for one such value of ξ', it must be true for $S_{N'}$ terms in the sum total, since that is how many times N' is mapped to itself through a translation by ξ'. So when the sum is non-zero, it will be equal to $S_{N'}$. This, however, assumes that there will be such a translation ξ' that satisfies $\hat{T}_{\xi'}N' = \hat{T}_{\xi}N - n + n'$. So we assume that it does, name it γ, and add a Kronecker delta to check for the possibility. In particular,

$$\sum_{\xi'} \langle 0|\hat{A}_{N'}\hat{T}_{\xi'}\hat{A}^{\dagger}_{T_{\xi}N-n+n'}|0\rangle = S_{N'}\boldsymbol{\delta}_{\hat{T}_{\gamma}N',\hat{T}_{\xi}N-n+n'} = S_{N'}\prod_{x}\delta_{N'_{x-\gamma},N_{x-\xi}-n_x+n'_x} \ . \tag{B.9}$$

This allows us to further simplify our end goal in B.8 to

$$\begin{aligned}\langle \bar{\boldsymbol{N}}'|\mathcal{O}(\boldsymbol{n}',\boldsymbol{n})|\bar{\boldsymbol{N}}\rangle = \frac{1}{L}\sqrt{\frac{S_{N'}}{S_N}}\sum_{\xi}\left[\prod_{x}\theta(N_{x-\xi}-n_x)\sqrt{\frac{N_{x-\xi}!\ (N_{x-\xi}-n_x+n'_x)!}{(N_{x-\xi}-n_x)!\ (N_{x-\xi}-n_x)!}}\right] \\ \times\prod_{x}\delta_{N'_{x-\gamma},N_{x-\xi}-n_x+n'_x} \ .\end{aligned} \tag{B.10}$$

But now we can rewrite all terms containing ξ with the Kronecker delta, allowing us to move everything through the sum over ξ except for the Kronecker delta itself:

$$\begin{aligned}\langle \bar{\boldsymbol{N}}'|\mathcal{O}(\boldsymbol{n}',\boldsymbol{n})|\bar{\boldsymbol{N}}\rangle = \frac{1}{L}\sqrt{\frac{S_{N'}}{S_N}}\left[\prod_{x}\theta(N_{x-\gamma}-n'_x)\sqrt{\frac{(N'_{x-\gamma}-n'_x+n_x)!\ (N'_{x-\gamma})!}{(N'_{x-\gamma}-n'_x)!\ (N'_{x-\gamma}-n'_x)!}}\right. \\ \left.\times\sum_{\xi}\delta_{N'_{x-\gamma},N_{x-\xi}-n_x+n'_x}\right] \ .\end{aligned} \tag{B.11}$$

Like before, this final sum is only non-zero when there exists some σ for which $\hat{T}_{\gamma}N' = \hat{T}_{\sigma}N - n + n'$. If no such σ exists, then the whole matrix element is zero. If it does, then there will be exactly S_N non-zero terms in the sum, all equal to one. So we again assume there does exist a σ, and edit the Kronecker delta to account for the zero possibility. Our

whole matrix element then becomes

$$\mathcal{O}(\boldsymbol{n}', \boldsymbol{n})_{\bar{\boldsymbol{N}}', \bar{\boldsymbol{N}}} = \frac{\sqrt{S_{N'} S_N}}{L} \left[\prod_x \theta(N_{x-\gamma} - n'_x) \sqrt{\frac{(N'_{x-\gamma} - n'_x + n_x)!\ (N'_{x-\gamma})!}{(N'_{x-\gamma} - n'_x)!\ (N'_{x-\gamma} - n'_x)!}} \delta_{N'_{x-\gamma}, N_{x-\sigma} - n_x + n'_x} \right], \tag{B.12}$$

as stated in equation 2.14. To recap, the theta functions remind us to check for a translation γ such that for all lattice sites x we have $N_{x-\gamma} - n'_x \geq 0$, and the Kronecker deltas remind us to check that there must also be a σ such that for all lattice sites x we have $N'_{x-\gamma} = N_{x-\sigma} - n_x + n'_x$. If these conditions are not met, the matrix element is then 0. This is the "computationally efficient" way to understand these matrix elements.